Fault reactivation by stress pattern reorganization in the Hyblean foreland domain of SE Sicily (Italy) and seismotectonic implications

Fabrizio Cultrera [a], Giovanni Barreca [a], Luciano Scarfì [b], Carmelo Monaco [a]

[a] Dipartimento di Scienze Biologiche, Geologiche e Ambientali, Università di Catania, Sezione di Scienze della Terra, Catania, Italy

[b] Istituto Nazionale di Geofisica e Vulcanologia, Osservatorio Etneo, Catania, Italy

Corresponding author: Fabrizio Cultrera

e-mail: fcultrera@unict.it

fax: +39 0957195728

Keyword: Hyblean foreland, seismic sequences, fault reactivation, 3D fault modelling, stress changing, seismotectonics

Abstract

Between the October 2011 and the July 2012, several seismic swarms occurred in the Hyblean foreland domain of SE Sicily (Italy) along the Cavagrande Canyon, one of the most impressive fluvial incisions of Sicily. Despite the low magnitude of the events (main shock with M~3.7), they represent the biggest strain release of the Hyblean area over the last ten years. A careful wave-form analysis of the earthquakes revealed that most of them form a family of "multiplets". These findings allow us to reconstruct the attitude of the accountable fault plane by interpolating their high-precision 3D location parameters into a GIS platform. A detailed morpho-structural analysis, performed at the ideal updip projection of the modelled plane, showed that during the Middle-Late Pleistocene the epicentral area has been deformed by a belt of extensional faults, a segment of which matches well with the computer-generated surface. Despite the field evidence, computed focal solutions support contrasting strike-slip kinematics on the same fault plane, clearly indicating a dextral shearing on this pre-existing normal fault. The seismic swarms nucleated on a small rupture area along a ~10 km long, NW-SE trending fault segment, that could be able to generate M~6 earthquakes. Following our analysis and looking at seismicity distribution in the SE portion of Hyblean area, we asses that a stress pattern reorganization occurred all over the Hyblean foreland between the Late Pleistocene and present-day. Change in the trajectory of the max stress axes (from vertical to horizontal) seems to have involved a pre-existing large scale fault configuration with considerable seismotectonic implications.

1. Introduction

Fault reactivation under different stress conditions has been documented by several authors in various tectonic settings (Bonini et al., 2012; Viola et al., 2004; Richard and Krantz, 1991; Koopman et al., 1987). This process is commonly interpreted as the expression of a changed tectonic regime or as the result of local stress perturbation. Reactivation is a selective process which, in many cases, reworks pre-existing zones of rheological and mechanical weakness (Holdsworth et al., 2001) since it is mechanically easier than forming a new fault (Scholz, 1998). Previously faulted zone can also influence the kinematic pattern and the strain accumulation with associated seismicity depending on the geometric relations between re-oriented stress and trend of inherited faults. In particular, when the trend of the pre-existing faults is nearly perpendicular or oblique to the orientations of maximum horizontal stress, high angle dip-slip faults are prone to be reactivated as strike-slip mode rather than reverse one (Davis and Reynolds, 1984; Letouzey et al., 1990). Moreover, analog sandbox experiments showed that reactivation in strike-slip mode of pre-existing faults can occur at depth without surface expressions (Richard and Krantz, 1991).

The Hyblean Plateau is an highly-fractured carbonate block of SE Sicily (southern Italy) which experienced several deformation phases during Neogene-Quaternary times (Grasso and Lentini, 1982). The main tectonic features consist of extensional fault systems, widespread all over the Hyblean area, which mainly nucleated in response to foreland-bulging dynamics within a larger geodynamic scenario dominated by the long-living convergence between Nubia and Eurasia plates (Faccenna et al., 2001; Dewey et al., 1989). These NE-SW oriented faults generally occur at the edges of the Hyblean Plateau block, whereas other fault systems, mainly NW-SE trending, dissect its internal portion. As suggested by the occurrence of several destructive seismic events and sequences in historical times (e.g. the 1169 and 1693 earthquakes, MCS intensities of XI with estimated magnitudes of about 7 or higher; Boschi et al., 2000) faulting is still active, even though the lack of coseismic ruptures at surface (or not found yet) and other clues that typically develop in a seismic landscape (sensu Michetti et al., 2005) makes the location of the seismogenic sources for these large earthquakes problematic.

Apart from the well-known extensional tectonics, oblique deformation has also been documented in the Hyblean Plateau and particularly at its western sector (Grasso and Reuther, 1988; Ghisetti and Vezzani, 1980), where reactivation in strike-slip mode of pre-existing normal faults system has been evidenced (Monaco et al., 2003). Recent seismological and geodetic studies (Musumeci et al., 2014) indicate that the entire Hyblean Plateau is currently undergoing prevailing strike-slip deformation. This kinematic pattern has been interpreted by the authors as the result of foreland

segmentation dynamics even though the geological expression of this ongoing processes and correlation between seismicity and the accountable tectonic structures have not been satisfactorily explored.

Starting from the analysis of low-magnitude seismic swarms recently occurred in the southern portion of the Hyblean Plateau (the 2011-2012 Cavagrande seismic sequence), we firstly provide a GIS-aided method to model the attitude of the responsible fault surface (or the geometry of the asperity where rupture nucleated) by managing high-precision locations of a family of multiplet earthquakes, i.e. a group of events with similar waveforms detected within a considered seismic cluster. Results have been after matched with a detailed morpho-structural analysis at the ideal updip projection of the modelled plane. The comparison between seismological and field data allows us to capture the instrumental and the morpho-structural signatures of recent stress pattern configuration along this sector of the Hyblean Plateau and to identify a seismogenic structure resulting from tectonic reactivation.

2. **Geodynamic setting**

2.1 General outlines

The Hyblean Plateau (hereinafter the HP) is an isolated carbonate "promontory" in the central Mediterranean region which represents the emergent fragment of a larger foreland domain, the Pelagian Block (Burollet et al., 1978, Ben-Avraham and Grasso, 1991, Fig. 1A). This is a ~ 25-30 km thick continental crustal portion of the African margin (Cassinis, 1983; Scarascia et al., 1994; Dewey et al., 1989), extending from the Sahel region of Tunisia to the eastern Sicily, where it is interrupted by the Malta Escarpment, a regional tectonic boundary that separates the Pelagian Block from the Ionian Basin (Nicolich et al., 2000; Torelli et al., 1998, Fig.1A). As revealed by the long-time collected field and sub-surface data, the HP is formed by ~10 km thick Mesozoic-Cenozoic carbonate sequences with several intercalations of volcanic products (Patacca et al., 1979; Grasso et al., 2004). Exposed rocks consist of Cretaceous to Miocene shallow to open-shelf series outcropping in the eastern and western sector, respectively (Grasso and Lentini, 1984, Fig. 1B). Top-sequences are made up of Quaternary sediments, generally preserved within fault-bounded structural depressions at the edges of the HP, and lava flow units mostly outcropping at its northern border (Grasso and Lentini, 1984).

The deformation history of the HP has been conditioned by its crustal feature (Barreca, 2014) and by the foreland role that it played within the larger geodynamic scenario dominated by the NW-SE convergence between Nubia and Eurasia plates (Faccenna et al., 2001; Dewey et al., 1989). During the Neogene, the progressive tectonic shortening has involved the northern portion of the

Pelagian Block, giving rise to a NE-SW trending, foreland-verging fold and thrust system (the Sicilian Collision Zone, SCZ in Fig. 1B) During this phase, thrust sheets piled at the north-western margin of the underthrusted Hyblean foreland, causing tectonic overload and consequent foreland-bulging of the HP (Billi et al., 2006). This process developed since the middle Miocene time (Grasso and Pedley, 1990) and has reached its acme (probably) during the late Miocene-early Pliocene when deep-thrusting of previously flexured foreland units occurred in the inner part of the SCZ (Catalano et al., 2013). Bulging produced the large bending of the HP, with the consequent development of a gentle NE-SW trending hinge zone (roughly parallel with the trend of the SCZ), accompanied by extensional tectonics along coaxial outer-arc fault systems (Grasso et al., 1995) and by the nucleation of pervasive fracture systems with orthogonal trends (NW-SE and NE-SW respectively, see Billi et al., 2006).

More recently, regional and fault-related uplift, accompanied by sea level changing, caused episodic emersions of the HP, as testified by the occurrence of several orders of Pleistocene marine terraces (Bianca et al., 1999 and reference therein) culminating with a large (~480 ky old, according to Bianca et al., 1999) wave-cut summit surface, presently exposed on the eastern part of the HP.

2.2 Tectonic setting of the Hyblean Plateau

In contrast with the deformation expected by the foreland-bulging dynamics (outer-arc extensional fracturing, parallel to the NE-SW oriented hinge zone, see above), the HP exhibits a network of variously oriented fault systems, mostly extensional and subordinately strike-slip. Eastwards, the HP ends with the Malta Escarpment system (Fig. 1A and B), a ~NNW-SSE trending normal to oblique fault belt partially reactivating the ancient (Mesozoic) boundary between the HP and the adjacent Ionian Basin (Scandone et al., 1981; Fabbri et al., 1982; Casero et al., 1984). Quaternary activity of this fault belt is testified by the occurrence of coaxial on-land graben structures (e.g. the Augusta structural depressions, Fig 1B), filled by Late Quaternary marine sediments (Bianca et al., 1999). The northern edge of the HP is controlled by a NE-SW trending extensional fault belt (the Monterosso–Agnone Fault System, MAFS in Fig. 1B) which has accommodated its northward bending beneath the front of the SCZ (Grasso and Pedley, 1990). Faulting gives rise to the setting of NE-SW oriented structural highs and depressions (e.g. the Scordia-Lentini Graben and the S. Demetrio High, Fig. 1B). The western border of HP is deformed by a system of NE-SW oriented extensional faults array, the Comiso-Chiaramonte Fault Belt (Ghisetti and Vezzani 1980; Grasso et al., 2000, Fig. 1B) through which the Hyblean successions have been downfaulted by about 4000 m (Cogan et al., 1989). Similarly to the northern border, the southern sector of the HP is dissected by a NE–SW oriented normal fault system which includes the

Pozzallo-Ispica-Rosolini Fault Belt and the ~20 km long Avola Fault (Grasso et al., 1992; Bianca et al., 1999; Monaco and Tortorici 2000). Apart from the NE-SW trending bounding faults, resulting from regional bulging process (Grasso et al., 2000), the HP is also internally deformed by ~N-S and NW-SE trending tectonic structures. The western portion is transversally sliced by a ~70 km long, roughly N-S oriented, shear zone, known as the Scicli-Ragusa Fault System (SRFS, Ghisetti and Vezzani, 1980; Grasso and Reuther, 1988, see Fig. 1B), which offset in right-lateral mode the bulging-related NE-SW structures. The NW-SE striking faults exclusively occur in the eastern part of HP within a rectangular-shaped deformation zone, confined between the Monterosso-Agnone Fault System to the north (MAFS in Fig. 1B) and the Pozzallo-Avola Fault System (PAFS in Fig. 1B), to the south. With respect to the fault systems that affect the northern edge, whose recent tectonic activity is demonstrated by displaced late Quaternary sediments, active deformation along the southern ones remains doubtful (see Bianca et al., 1999).

2.3 Seismotectonics

The Hyblean Plateau is one of the most seismically hazardous region of Italy since it has been struck by large earthquakes in historical times such as the February 4, 1169 and the January 11, 1693 events. The latter is commonly reported as the strongest seismic event of the Italian Peninsula (Io = X/XI MCS and Mw 7.4 according to CPTI04 reference catalogue, see Fig. 2A for the inferred epicentral locations), causing more than 54.000 casualties and extensive damages in the whole Eastern Sicily (Bianca et al., 1999; Visini et al., 2009 and reference therein). The location of its seismogenic source is a topic still widely debated: normal-oblique faults located along the Ionian offshore (e.g. Piatanesi and Tinti, 1998; Bianca et al., 1999; Gutscher et al., 2006; Visini et al., 2009; Argnani et al., 2012) and/or compressional structures located to the north and to the south of the Catania Plain, between the front of the Appenninic–Maghrebian Chain and the northern margin of the Hyblean foreland (e.g. DISS Working Group, 2015). According to Bianca et al. (1999), the major foreshock of this event, characterized by MCS intensity of VIII–IX (Boschi et al., 2000), could have nucleated along the PAFS. More recently, a M_L = 5.4 earthquake occurred on December 13, 1990, about 10 km offshore from the northeastern edge of Hyblean Plateau (Amato et al., 1995). The current seismotectonic setting of the HP is well depicted by the seismic activity (Fig. 2A), characterized by low to moderate magnitudes ($1.0 \leq ML \leq 4.6$) and hypocentral depths in the range of 15-25 km (Musumeci et al., 2014). Even though the earthquakes appear scattered all over the Hyblean area, a number of events seems to follow the major tectonic structures, the Scicli-Ragusa Fault System, to the west, and the northern segment of the Malta Escarpment to the east.

Nevertheless, in the last 20 yrs (1994-2013, "Catalogo dei Terremoti della Sicilia Orientale–Calabria Meridionale", http://www.ct.ingv.it/ufs/analisti/catalogolist.php) the highest number of earthquakes (Fig. 2B) has occurred within the rectangular-shaped region between the overlapping NE-SW oriented MAFS and PAFS (see also section 2.1 and Fig. 1B). Here, the epicentral distribution seems to concentrate along the NW-SE faults and less along the bounding NE-SW oriented structures, whereas no seismicity is recorded north of the MAFS and south of the PAFS (see Fig. 2A). Available focal solutions (Musumeci et al., 2014) indicate that seismogenic faulting in the HP mainly occurs on strike-slip, subordinately normal and rarely reverse ruptures, the latter along the NE-SW oriented PAFS.

3. The 2011-2012 Cavagrande seismic swarms

3.1 Seismological features

Most of the seismicity located in the narrow sector of the Cavagrande Canyon is clustered at its western tip and is related to two main seismic sequences occurred between October 2011 and July 2012. Each sequence encompasses hundreds of small magnitude earthquakes ($1.0 \leq M_L \leq 3.7$), i.e. as much as 560 events. Despite their low magnitude, the sequences represent the biggest strain release in the Hyblean area over the last ten years (D'Amico et al., 2014). Such seismicity pattern is unusual for the Hyblean area, having been recorded few times to date. In particular, micro-earthquakes swarms with a considerable number of events occurred in November 1999 and January 2000, about 20 km SW of Mt. Etna (Scarfì et al., 2003), and in 2002, close to the 1990 earthquake epicentral area (Brancato et al., 2009).

Locations of the 2011 and 2012 sequences indicate the activation of a seismogenic volume, depicting a WNW-ESE to NW-SE trend, similarly to other seismic clusters located in the surrounding areas of the Hyblean Plateau (Musumeci et al., 2014). Accordingly, focal solutions (see Fig. 3A) indicate right-lateral movements on the same direction. Hypocentral depth was found ranging between 5 and 10 km b.s.l., whereas typical seismogenic depths of the Hyblean Plateau are between 15 and 25 km (Musumeci et al., 2014). Due to the quite shallow hypocenter (8 km), the ML=3.7 strongest event, occurred on 27 June 2012, was widely felt in the Hyblean area up to Catania, about 60 km far from the epicenter, and it caused slight damages in the surrounding towns. Historical dataset (CPTI11 by Rovida et al., 2011) revealed that the same area was shaken by a M=4.5 event in 1696, the epicentral location of which is reported very close to seismic swarms here analyzed.

3.2 Fault plane modelling

On a scale of a few kilometres or less, the correlation between a seismicity pattern and the accountable tectonic structure is often difficult, since errors in standard location procedures may blur the real geometry of seismogenic features or create unnatural patterns (e.g., Scarfì et al., 2005). However, substantial improvements in precision of earthquake locations can be obtained when event-clustering techniques are used to get more accurate arrival-time estimates (e.g., Rowe et al., 2004; Scarfì et al., 2003, 2005).

In our case, a careful analysis of the events located in the investigated area revealed that most of the Cavagrande earthquakes form a family of events with similar waveform signatures, called "multiplet events", which are commonly interpreted as due to repeated slip on the same fault plane (e.g., Tsujiura, 1983-a, b; Nishigami, 1987). Their location can be defined by relative location procedures, where one focuses on spatial offsets between earthquake hypocentres rather than their absolute position. This allows an high precision, in the order of few meters, enabling to investigate small tectonic features. In practise, the general strategy of this technique consists of locating the position of a "slave" earthquake relative to a reference "master" event by determining accurately their P- or S-wave travel-time differences at the same stations. Following the method proposed by Fremont and Malone (1987) (see Scarfì et al., 2003, 2005 for further details about the procedures), we were able to relocate with great accuracy a dataset of 42 well-recorded multiplet events (Tab. I). Assuming that the 3D spatial distribution of a clustered earthquake sequence may mimic the geometry of the active fault from which the events nucleated, we tried to model the tectonic structure responsible for the Cavagrande Canyon earthquake cluster. We proceeded by handling the relocated multiplets into a GIS software as points features. Geographic coordinates and hypocentral depth (x, y and z attributes) were used as cloud of points for surface generation that has been produced by applying "Trend" and "Natural Neighbor" interpolation methods (Sibson, 1981; Watson, 1992). In the first case, the resulting plane consists of a smoothed best-fit surface not necessary passing through all the points whereas in the second one, a manifold surface, that follows the real spatial position of the input data point, has been generated. From each modelled surface we derived the relative aspect (the dip-direction) and slope (the dip-degree) representation, hence the attitude of the fault plane/asperity where rupture nucleated.

Trend interpolation methods provided a N97E trending surface plunging at ~77,5° towards the SSW, with an areal extension of ~20 km ^{2} (Fig. 3B-1). Similarly, natural neighbor interpolation provided a N99E oriented plane plunging in average at 77° towards the SSW. The obtained trend is

the average value of the attitude calculated for all the minor cells forming the whole manifold surface (Fig. 3B-2).

4. Field data

4.1 Fault and fracture systems

To test the workflow used for reconstructing the 3D fault plane/asperity geometry, we undertaken a detailed field analysis of the area, in particular along the ideal updip projection and possible intersection with the topographic surface of the modelled fault plane and in the nearby (see Fig. 3C). Middle-Upper Miocene carbonate sediments, locally known as "Palazzolo Formation" (Di Grande et al., 1982), are here largely exposed with near-horizontal strata attitude. As evidenced by previous workers (Catalano et al., 2010; Grasso and Lentini, 1984; Di Grande et al., 1982), the area is mainly deformed by a WNW-ESE to NW-SE oriented fracture system (Figs. 4A and 5A-B). It forms a major extensional fault belt (the Canicattini Fault Belt, CFB in Fig. 4A) which extends for about 15 km from the Avola fault, to the SE, to the Canicattini village, to the NW. These faults show ~N-facing and 70-80° dipping scarps that in places reach height of 150 m. Structural measurements evidenced pure extensional motion along some fault planes (see below).

Southwards, field surveys evidenced a series of tectonic structures forming another tectonic belt, here called the Cavagrande Fault Belt (CGFB in Fig. 4A), that consists of WNW-ESE to NW-SE trending fault segments, forming horst and graben structures. NW-SE striking segments affect the NW portion of the Cavagrande river basin, giving rise to a narrow (~2 km wide) structural depression near the epicentral area. The NE side of the graben, roughly corresponding to the zone at the ideal updip of the modelled fault plane (see section 3.2), is controlled by a ~10 km long, N130E trending fault (the red segment in Fig. 4A), dipping towards the SW of ~75°. At a more detailed scale, the tectonic structure consists of three fault segments with bell-shaped scarps connected by a series of variously oriented joints and calcite filled fractures (Fig. 5C). Faults kinematic has been inferred by slickenlines analysis, which suggested a pure extensional motion (pitch 90-100°, station 37) for these structures. Fault scarps reach the maximum height of about 80 m (Fig. 4B) that progressively reduces at their tips (e.g. ~0.3 m offset at the south-eastern segment, Fig 4C and station 15). The SW side of the structural depression is characterized by the occurrence of a segmented fault system, of which the major structure consists of a WNW-ESE trending extensional fault that exhibits a NE-facing scarp, reaching the height of ~ 80. Also in this case, height variation gives rise to along-strike bell-shaped scarp at the footwall, whereas tilting of the hanging-wall block towards the fault is observed. .

Eastwards, a belt of *én-echelon* arranged faults affects the eastern and deeper part of the Cavagrande Canyon. Faults are mostly characterized by NNE-facing, left-stepping WNW-ESE trending segments down-faulting the northern shoulder of the Canyon of about 50 m (see section 4.3). The overlap sectors between the various segments form narrow relay zones characterized by the occurrence of 5-10 m spaced NE-SW to NNE-SSW oriented extensional joint systems (see inset 2, Fig. 4A for model and Fig. 5D).

Even though all segments of the CGFB do not exhibit clear kinematic indicators, the vertical displacement and the dipping towards the respective hanging-walls of the fault planes suggest that they can be interpreted as extensional structures with a prevailing normal sense of motion. This is confirmed by a geological cross section (inset 1 in Fig. 4A) constructed by using available commercial boreholes (e.g. the Avola1 and Siracusa1 wells; http://unmig.sviluppoeconomico.gov.it/deposito/pozzi, see Fig. 4A for locations) and others wells available from groundwater research. Using as a marker line the bottom of the Palazzolo Formation, vertical displacements of 50-80 m and of ~ 300 m have been estimated for the CGFB and the CFB, respectively.

Nevertheless, as exposed above, focal solutions provided for the Cavagrande seismic sequences (see section 3) indicate a near-strike slip faulting mechanism. To understand this discrepancy we performed a detailed meso-structural analysis for better constraining the kinematics of the faults, mainly focusing on the structures mapped near the epicentral area and along the Cavagrande Canyon.

4.2 Mesostructures and fault kinematics

Mesostructural data have been collected on 42 sites of measurements (Fig. 5A) and consist of mesofaults and prevailing fractures with distinct azimuthal distribution. Slip vectors along fault planes have been obtained by steps, Riedel fractures, tecto-grooves and, rarely, slickensides. Data have been represented by using Schmidt lower hemisphere convention. Mesofaults consist of sub-vertical normal dip-slip and rare strike-slip structures. Dip-slip mesofaults are distributed all over the area, forming WNW-ESE to NW–SE oriented (N100-120E, see rose diagram in Fig. 5B) extensional or slightly oblique (right-lateral, see plot 19 in Fig. 5A) systems that are roughly coaxial to the trend of the main faults. Doubtful left-lateral motion has been also observed on NE-SW trending (N30–50E) mesostructures (plots 14,15, 19 and 30 in Fig. 5A), slicing transversally the Cavagrande Canyon.

Fracture systems consist of pervasive sets of joints and calcite-filled fractures/veins (Fig. 5C) distributed into two distinct azimuthal domains. The most represented set (35.5 % in the N30-50E range, see rose diagram in Fig. 5B) is characterized by a system of closely-spaced fractures (Fig. 5D) with sub-vertical (85–90°) planes attitude. A minor set of fractures consists of N110-125E oriented extensional joints, mainly observed along the footwall of the major faults (Fig. 5E).

As a whole, the WNW-ESE to NW-SE oriented fracture systems follow the trend of major faults and can be interpreted as "fault-parallel-joints" (Mode I fractures, see Peacock, 2001; Hancock, 1985; Anderson, 1951). Conversely, the NE-SW trending discontinuities form high-angle with the trend of the main faults and can be interpreted as extensional "cross joints" (see Bai et al., 2002; Kattenhorn et al., 2000; Engelder and Gross, 1993; Rawnsley et al., 1992). Even though these joint and veins systems are widespread all over the area, they have been mainly recognized within narrow damaged sectors at the overlapping zones between the *én-echelon* arranged fault segments (e.g. those parallel to the Cavagrande Canyon, see section 4). Although less represented, NE-SW trending joints have also been measured away from the overlapping/relay zones. Cross-cutting relations revealed that the NE-SW trending joints propagates across or terminate against the NW-SE oriented main faults, forming with them a grid of interconnected mechanical discontinuities (Fig. 4A-2 and 5D). Dipping of major fault planes towards the respective down-bended hanging-walls, bell-shaped footwall scarps and rare slickensides observed along the Canicattini Fault Belt, in general suggest an overall extensional regime for the CGFB.

4.3 Clues of recent tectonic from morphological signatures

Since measured faults and joints propagated within the ~5 Ma old limestones of the Palazzolo Formation (Serravallian-Messinian) and recent deposits are lacking, we used an high-resolution DTM (2x2 m cell size) to detect possible morphological signatures of the recent tectonic activity. This sector of the Hyblean Plateau is characterized by a regional slope plunging at 11.5° towards N150E direction. Accordingly, this morphological setting has controlled the orientation of fluvial paths that generally flows along the same direction and frequently within structural depressions. Conversely, the Cassibile River (Fig. 6A) exhibits two distinct orientations of its main course, N145E in the upstream of its catchment (according to regional slope) and N105E along the Cavagrande Canyon. Changes in the river stream direction occur near the epicentral area where the Cassibile river is barred by the WNW-ESE trending, ~80 m-high fault scarp (see section 4.1). The fault-wall seem to have caused river deflection (Fig. 6A) and its channeling along the N105E direction.

Evidences of recent tectonic control on the fluvial morphology are also suggested by the execution of series of high-precision topographic profiles (see inset in Fig. 6A) across the Cavagrande Canyon. The profiles clearly show that the southern shoulder of the canyon is in average 50 m higher than to the northern one, suggesting the occurrence of a canyon-parallel extensional displacement (see section 4.1, and Fig. 6B) displacing the Middle Pleistocene summit surface (see Section 2.1 and profile A-A' in Fig. 6A). The activity of such canyon-parallel fault system gave rise to the down-bending of the hanging-wall (Fig. 6C) that also involved the topographic surface (see also the profile E-E' in Fig. 6A). This deformation probably caused channel migration towards the main fault-wall and abandonment of meanders (Fig. 6D). This fluvial setting resembles previous model on rivers morphology controlled by recent tectonic activity (Leeder and Alexander, 1987). Along the Cavagrande Canyon, fault activity was accompanied by the growth of fault-parallel ridges (the modern watershed) that superimposed on ancient NNW-SSE oriented fluvial ridges and streams (Fig. 6E). Evidence of recent tectonic activity are also suggested by straight fault scarps that show at any scale values of mountain-front sinuosity index (Bull and McFadden, 1977) ranging from 1 to 1.2 which sometime dislocate karst morphologies (e.g. kamenitza, Fig. 5F).

5. Analysis of data

The identification of a number of multiplets within the low-magnitude seismic swarms recently occurred in the SE sector of the Hyblean Plateau, gave us the opportunity for 3D modeling of the accountable fault plane. Multiplets are in fact considered as generated by subsequent ruptures on the same tectonic structure (Tsujiura, 1983-a, b; Nishigami, 1987). Applying into a GIS-system of common interpolation methods (e.g. trend and natural neighbor algorithms) on the location attributes (x, y, and z) of high-accuracy relocated multiplets provides a WNW-ESE trending surface (N97-99E), whereas "aspect" and "slope" algorithms on the generated plane provide the dip-direction (toward the SSW) and the dip-degree (77°), respectively. The seismic rupture occurred at depths ranging between 5 and 10 km, over an area of ~ 20 km^2. The derived surface attitude is in accordance with the geometry of major outcropping extensional faults. In particular, the ideal updip projection of the modelled fault plane matches well with an exposed fault which exhibits a bell-shaped footwall scarp along-strike, with maximum height of ~80 m. The latter constitutes an antithetic fault segment whit respect to the *én-echelon* arranged, WNW-ESE trending fault system belonging to the Cavagrande Fault Belt (CGFB in Fig. 4A).

As for other fault belts of the Hyblean Plateau, the CGFB appears to be characterized by normal dip-slip movements evidenced by high-resolution topographic profiles across the river canyon (Fig. 6A), whose southern shoulder lies at ~50 m further up with respect to the northern one. Although these faults only involve middle-upper Miocene sediments, a recent (middle-Late Pleistocene) activity by normal faulting is suggested by the occurrence of i) displaced summit surface (attributed to ~ 480 ky ago, by Bianca et al., 1999; Fig. 6A) and straight fault scarps that at any scale show low values of mountain-front sinuosity index (1-1.2) which sometime dislocate karst morphologies (e.g. kamenitza, Fig. 5F), ii) river stream deflections near the epicentral area and iii) abandoned meanders on the bended hanging-walls. The impressive fluvial incision (~ 300 m depth) that characterizes the Cavagrande Canyon also implies a large-scale uplift of the region, probably related to a simultaneous activity of the major Avola Fault (see also Bianca et al., 1999). Despite field evidence, computed focal solutions for the Cavagrande seismic sequence (see section 3 and Fig. 3A) indicate a contrasting right-lateral strike-slip motion on the WNW-ESE modelled fault planes and reverse kinematic on NE-SW oriented nodal planes. This discrepancy suggests that the pre-existing WNW-ESE to NW-SE striking extensional faults have been recently reactivated in strike-slip mode. This process can be related to a stress pattern reorganization, as corroborated by *in-situ* tectonic stress measurements at the Capo Negro 1 and Cassibile 1 wells (Ragg et al., 1999, see Fig. 4A for location), that provide a local N166E direction for the max stress axis, i.e. geometrically favorable to a dextral shearing on the WNW-ESE to NW-SE oriented CGFB.

As a whole, borehole breakouts (Ragg et al., 1999) and P-axes obtained by focal mechanisms trending (Musumeci et al., 2014) suggest that NNW-SSE trending max stress axis can be considered as a stress-state currently acting in the Hyblean Foreland. Further, seismological (Neri et al., 2005) and geodetic data (Ferranti et al., 2008; Mattia et al., 2012) indicate that, northwards, the SCZ is itself shortened by a max stress axis with similar trend; such a stress pattern is also confirmed by field structural data (Barreca et al., 2010; Billi et al., 2010; Barreca and Maesano, 2012; De Guidi et al., 2015). In this framework, the NNW-SSE oriented σ1, involving both the SCZ and the HP and responsible for the deep thrusting of previously flexured foreland units (Catalano et al., 2013), has conceivably determined the reactivation in strike-slip and reverse mode of the Hyblean tectonic structures.

6. Seismotectonic implications

Evidences of tectonic reactivation have been documented along the CGFB which, in turn, is part of a WNW-ESE to NW-SE oriented fault system developed within a rectangular-shaped crustal

block at the SE portion of the HP. It is noteworthy that the WNW-ESE to NW-SE oriented fault system occur only in this portion of the HP and it appears confined between two major NE-SW oriented bounding faults (the MAFS and PAFS, see Fig. 1B). There are at least two models explaining this type of fault configuration: i) a releasing zone between left-stepping, left-lateral strike slip bounding faults (see Sylvester, 1988 for an overview on strike-slip zone geometries) or ii) a transfer zone composed of an array of extensional connecting faults between two main overlapping hard-linked extensional bounding structures with opposite dip-polarity (inset in Fig. 7A; see Morley, 1988; Morley et al., 1990; Bose and Mitra 2010 for models). We exclude the first case since strike-slip deformation implies structural rotations at overstepping zones; indeed, paleomagnetic studies (Speranza et al., 1999) define the HP as an un-rotated/stable block. Conversely, the second hypothesis appears the most convincing kinematic configuration, in which a Middle-Late Quaternary transfer zone, composed of linkage faults (including the CGFB), developed at ~45° (the most common angular value reported in several models of transfer zone, see McClay, 1995 and Morley et al., 1990) to the trending of the two larger extensional fault systems. We call this sector the Hyblean Transfer Zone (HTZ in Fig. 7A). Faults connection is suggested by their inferred simultaneous activity during the Middle-Upper Pleistocene (e.g. on the CGFB and Avola Fault, see section 5).

Following our analysis and looking at seismicity distribution in the SE portion of HP (see also Fig. 2A), a recent reactivation seems to involve Pleistocene fault configuration. The occurrence of a current far-field and near-horizontal NNW-SSE oriented max stress axis should implies tectonic inversion on NE-SW trending faults and fracture systems (e.g. MAFS and associated structures, see Bonforte et al., 2014) and dextral shearing along the ancient WNW-ESE to NW-SE trending connecting structures (e.g. the CGFB). This recent seismotectonic setting (Fig. 7B) is suggested by i) right-lateral and left-lateral strike-slip solutions within the HTZ (Musumeci et al., 2014) and along the SRFS, respectively, ii) by geodetic contraction (~ 4,4 mm/yr; Mattia et al., 2012; Palano et al., 2012) at the northern edge of the Hyblean Plateau (i.e. along the MAFS) and iii) by the alignment of several NE-SW striking nodal planes with reverse kinematics roughly following the PAFS, southwards (Musumeci et al., 2014).

Furthermore, boreholes breakout data (Ragg et al., 1999, see black arrows in Fig. 7B) clearly depict a contractional setting near the PAFS with a NNW oriented near-horizontal max stress axis roughly orthogonal to the strike of the PAFS. Contraction along PAFS is also corroborated by coaxial Quaternary folds systems developed at its hanging-wall (Grasso et al., 1992). Accordingly, a rate of the contractional strain along the deep reactivated front of SCZ (named Sicilian Basal

Thrust, by Lavecchia et al., 2007, SBT in Fig. 7B) could be to date transferred in the still thrust-uninvolved Hyblean foreland.

6. Conclusion

Structural and seismological data from the Hyblean foreland, in SE Sicily, allow us to provide evidence for tectonic reactivation of a pre-existing fault belt. This latter consists of an ancient (likely Middle-Late Pleistocene) *én-echelon* arranged extensional fault system, which mostly developed parallel to the WNW-ESE oriented Cavagrande Canyon, one of the most impressive fluvial incision of Sicily and the deepest of the Hyblean Plateau. Fault plane modelling and focal solutions revealed that a ~ SSW-dipping, WNW-ESE trending surface, that is an attitude similar to that of several exposed normal fault scarps, is currently undergoing to a near-horizontal (~N140E) P-axis (see plot in Fig. 3A). This structure belongs to a Pleistocene WNW-ESE to NW-SE oriented fault system (the Cavagrande Fault Belt, CGFB). The geometric relations established between this inherited fault system and the newly-settled max stress axis, have created the favorable conditions for the reactivation of the CGFB in a dextral strike-slip mode and the consequent setting of a new seismogenic zone as revealed by the alongside intense seismicity.

The occurrence of a single generation of slickenlines along the outcropping fault planes (see picture in Fig. 4 A), indicating normal faulting, could be due to the lack of rupture propagation at surface during the newly-settled stress field. Taking into account that the analyzed seismic sequences have reactivated along-strike an antithetic segment of the CGFB, the new seismogenic zone could correspond to a ~10 km-long structure, reaching depths of about 9-10 km. This value represents the sum of the lengths of the various segments and of the associated relay zones (Kim and Sanderson, 2004). Using empirical fault-length scaling relationships (Wells and Coppersmith, 1994) and considering the seismogenic structure as continuous at depth (since it appears segmented at surface), we asses that the proposed seismogenic structure could be capable of generating M~6 earthquakes with a strong implication in the seismic potential of the region.

As already evidenced by Billi et al. (2010), this study confirm that eastern Sicily is a tectonically complex region where heterogeneous tectonic processes, generally related to Europa-Nubia convergence, coexist in a small area and sometimes give rise to reactivation of existing tectonic structures with different kinematics due to local stress pattern reorganization. This is the case of the reactivated HTZ and its nearby fault systems. An intriguing aspect is that the analyzed area is also the locus with the highest density of earthquakes of the entire HP. Accordingly, the HTZ and the nearby faults probably play a significant role in the regional seismotectonic framework, being the

sector where some historical destructive earthquakes (e.g. the 1125, 1542, 1990 events and the 1693 major foreshock) probably nucleated.

Acknowledgements

The authors would like to thank Stefano Gori and Andrea Billi for the accurate and constructive reviews of the manuscript. This work was funded by PRIN 2010-11 Project "Active and recent geodynamics of Calabrian Arc and accretionary complex in the Ionian Sea" (responsible C. Monaco).

References

Amato, A., Azzara, R., Basili, A., Chiarabba, C., Cocco, M., Di Bona, M., Selvaggi, G., 1995. Main shock and aftershocks of the December 13, 1990, Eastern Sicily earthquake. Ann. Geofis. 38, 255–266.

Anderson, E.M., 1951. The Dynamics of Faulting. Olivier and Boyd, Edinburgh, 206 pp.

Argnani, A., Armigliato, A., Pagnoni, G., Zaniboni, F., Tinti, S. and Bonazzi, C., 2012, Active tectonics along the submarine slope of south-eastern Sicily and the source of the 11 January 1693 earthquake and tsunami. Nat. Hazards Earth Syst. Sci., 12, 1311-1319. doi:l.5194/nhess-12-1311-2012

Bai, T., Maerten, L., Gross, M.R., Aydin, A., 2002. Orthogonal cross joints: do they imply a regional stress rotation? Journal of Structural Geology 24, 77–88.

Barreca, G., 2014. Geological and geophysical evidences for mud diapirism in south-eastern Sicily (Italy) and geodynamic implications. J. Geodyn., http://dx.doi.org/10.1016/j.jog.2014.02.003.

Barreca, G., Maesano, F.E., 2012. Restraining stepover deformation superimposed on a previous fold-and-thrust-belt: a case study from the Mt. Kumeta-Rocca Busambra ridges (western Sicily, Italy). Journ. Geodynamics, 55, 1-17, doi: 10.1016/j.jog.2011. 10.007.

Barreca, G., Maesano, F.E., Carbone, S., 2010. Tectonic evolution of the Northern Sicanian-Southern Palermo Mountains range in Western Sicily: insight on the exhumation of the thrust-involved foreland domains. Ital. J. Geosci. (Boll. Soc. Geol. It.), 129 (3), 234-247.

Ben-Avraham, Z., Grasso, M., 1991. Crustal structure variations and transcurrent faulting at the eastern and western margins of the eastern Mediterranean. Tectonophysics 75, 269–277.

Bianca, M., Monaco, C., Tortorici, L., Cernobori, L., 1999. Quaternary normal faulting in southeastern Sicily (Italy): A seismic source for the 1693 large earthquake, Geophys. J. Int., 139, 370 – 394.

Billi, A., Presti, D., Orecchio, B., Faccenna, C., Neri, G., 2010. Incipient extension along the active convergent margin of Nubia in Sicily, Italy: Cefalù-Etna seismic zone. Tectonics 29, TC4026, doi:10.1029/2009TC002559.

Billi, A., Porreca, M., Faccenna, C., Mattei, M., 2006. Magnetic and structural constraints for the non-cylindrical evolution of a continental forebulge (Hyblea, Italy). Tectonics 25, TC3011. http://dx.doi.org/10.1029/2005TC001800.

Bonforte, A., Catalano, S., Maniscalco, R., Pavano, F., Romagnoli, G., Sturiale, G., Tortorici, G., 2014. Geological and Geodetic Constraints on the Active Deformation along the Active Northern Margin of the Hyblean Plateau (Se Sicily). Tectonophysics (2014), doi: 10.1016/j.tecto.2014.11.024

Bonini, M., Sani, F., Antonielli, B., 2012. Basin inversion and contractional reactivation of inherited normal faults: A review based on previous and new experimental models. Tectonophysics 522–523, 55–88.

Boschi, E., Guidoboni, E., Ferrari, G., Gasperini, P., Mariotti, D., Valensise, G., 2000. Catalogue of Strong Italian Earthquakes from 461 a.C. to 1997. Ann. Geof., 43, 609-868 and CD-ROM.

Bose, S., Mitra, S., 2010. Analog modeling of divergent and convergent transfer zones in listric normal fault systems. AAPG Bulletin, p. 1425-1452.

Bull, W., McFadden L., 1977. Tectonic geomorphology north and south of the Garlock Fault, California, Geomorphology in Arid regions, D. O. Doehring, (eds.). Publications in Geomorphology. State University of New York at Bingamton, 115-138.

Burollet, P.F., Mugniot, G.M., Sweeney, P., 1978. The geology of the Pelagian Block: the margins and basins of Southern Tunisia and Tripolitania. In: Nairn, A., Kanes, W., Stelhi, F.G., (Eds.). The Ocean Basins and Margins. Plenum Press, 4 B, pp. 331–339.

Brancato, A., Hole, J.A., Gresta, S., Beale, J.N., 2009. Determination of seismogenic structures in southeastern Sicily (Italy) by high-precision relative relocation of microearthquakes. Bull. Seismol. Soc. Am. 99 (3), 1921–1936.

Casero, P., Cita, M.B., Croce, M., De Micheli, A., 1984. Tentativo di interpretazione evolutiva della Scarpata di Malta basata sui dati geologici e geofisici. Mem. Soc. Geol. It. 27, 233–254.

Cassinis, R., 1983. The structure of the earth's crust in the Italian region. In: Wezel, F.C. (Ed.), Sedimentary Basins of Mediterranean Margins. Tectonoprint, Bologna, pp. 19–32.

Catalano, R., Valenti, V., Albanese, C., Accaino, F., Sulli, A., Tinivella, U., Morticelli, M.G., Zanolla, C., Giustiniani, M., 2013. Sicily's fold–thrust belt and slab roll-back: the SI.RI.PRO. seismic crustal transect. J. Geol. Soc. London, doi: 10.1144/jgs2012-099.

Catalano, S., Romagnoli, G., Tortorici, G., 2010. Kinematics and dynamics of the Late Quaternary rift flank deformation in the Hyblean Plateau (SE Sicily). Tectonophysics 486, 1–14. http://dx.doi.org/10.1016/j.tecto.2010.01.013.

Cogan, J., Rigo, L., Grasso, M., Lerche, I., 1989. Flexural tectonics of SE Sicily. J. Geodyn.11, 189–241.

D'Amico, S., Ferrari, F., Maiolino, V., Messina, A., Ursino, A., 2014. Studio preliminare di due sequenze di microterremoti accadute nel 2011 e nel 2012 nell'area dei Monti Iblei Orientali (Sicilia Sud-orientale – Italia). Atti 33° Convegno GNGTS, Bologna, 1: 61-66.

Davis, G. H., Reynolds, S. J., 1984. Structural geology of rocks and regions (2nd ed., 776 p). New York: John Wiley & Sons, Inc.

De Guidi G., Barberi G., Barreca G, Bruno V, Cultrera F, Grassi S, Imposa S, Mattia M, Monaco C, Scarfì L, Scudero S., 2015. Geological, seismological and geodetic evidence of active thrusting and folding south of Mt. Etna (eastern Sicily): revaluation of "seismic efficiency" of the Sicilian Basal Thrust. J. of Geodynamics, 90, 32–41, doi: org/10.1016/j.jog.2015.06.001.

Dewey, J.F., Helman, M.L., Turco, E., Hutton, D.H.W., Knott, S.D., 1989. Kinematics of the Western Mediterranean. In: Coward, M.P., Dietrich, D., Park, R.G. (Eds.), Alpine Tectonics Geol. Soc. Spec. Publ. 45., pp. 265–283.

Di Grande, A., Romeo, M., Raimondo W., 1982. Il Membro di Gaetani ed il Membro di Buscemi della Formazione Palazzolo: facies, distribuzione ed età. Bollettino della Società Geologica Italiana, 101(03), pp. 343-372.

DISS Working Group, 2015. Database of Individual Seismogenic Sources (DISS), Version 3.2.0: A compilation of potential sources for earthquakes larger than M 5.5 in Italy and surrounding areas. http://diss.rm.ingv.it/diss/, © INGV 2015 - Istituto Nazionale di Geofisica e Vulcanologia - All rights reserved; DOI:10.6092/INGV.IT-DISS3.2.0

Engelder, T., Gross, M.R., 1993. Curving cross joints and the lithospheric stress field in eastern North America. Geology 21, 817-820.

Fabbri, A., Rossi, S., Sartori, R., Barone, A., 1982. Evoluzione neogenica dei margini marini dell'Arco Calabro-Peloritano: implicazioni geodinamiche. Mem. Soc.Geol. It. 24, 357–366.

Faccenna, C., Becker, T.W., Lucente, F.P., Jolivet, L., Rossetti, F., 2001. History of subduction and back-arc extension in the central Mediterranean. Geophys. J. Int. 145, 809–820. http://dx.doi.org/10.1046/j.0956-540X.2001.01435.x.

Ferranti, L., Oldow, J.S., D'Argenio, B., Catalano, R., Lewis, D., Marsella, E., Avellone, G., Maschio, L., Pappone, G., Pepe, F., Sulli, A., 2008. Active deformation in Southern Italy, Sicily and southern Sardinia from GPS velocities of the Peri-Tyrrhenian Geodetic Array (PTGA). Boll. Soc. Geol. Ital. 127 (2), 299–316.

Fremont, M.J., Malone, S.D., 1987. High precision relative locations of earthquakes at Mount St. Helens, Washington, J. geophys. Res., 92, 10 223–10 236.

Ghisetti, F., Vezzani, L., 1980. The structural features of the Hyblean Plateau and the Mount Judica area (South-Eastern Sicily): a microtectonic contribution to the deformational history of the Calabrian arc. Boll. Soc. Geol. It. 99, 55–102.

Grasso, M., Pedley, H. M., Behncke, B., Maniscalco, R., Sturiale, G., 2004. Integrated the Neogene-Quaternary sedimentation and volcanism in the northern Hyblean Plateau (Sicily). In: Pasquarè, G., Venturini, C. (Eds.), Mapping Geology in Italy. APAT, Roma, pp. 159–166.

Grasso, M., Philps, B., Reuther, C. D., Garofalo, P., Stamilla, R., Anfuso, G., Donzella, G., Cultrone, G., 2000. Pliocene-Pleistocene tectonics on the western margin of the Hyblean Plateau and the Vittoria Plain, Mem. Soc. Geol. Ital., 55, 35–44.

Grasso, M., Miuccio, G., Maniscalco, R., Garofalo, P., La Manna, F., Stamilla R., 1995. Plio-Pleistocene Structural evolution of the western margin of the Hyblean Plateau and the Maghrebian foredeep, SE Sicily: Implications for the deformational history of the Gela Nappe, Ann. Tectonicae, 9, 7 – 21.

Grasso, M., Reuther, C.D., Tortorici, L., 1992. Neotectonic deformation in SE Sicily: The Ispica Fault, evidence of late Miocene-Pleistocene decoupled wrenching within the central Mediterranean stress regime. J. Geodynamics, v.16 No 1-2, pp 135-146.

Grasso, M., Pedley, H. M., 1990. Neogene and Quaternary sedimentation patterns in the northwest Hyblean Plateau (SE Sicily): The effect of a collisional process on a foreland margin, Riv. Ital. Paleontol. Stratigr., 96, 219 – 240.

Grasso, M., Reuther, C. D., 1988. The western margin of the Hyblean Plateau: A neotectonic transform system on the SE Sicilian foreland, Ann. Tectonicae, 2, 107 – 120.

Grasso, M., Lentini F., (Eds.), 1984. Carta geologica della Sicilia sud-orientale, SELCA, Florence, Italy.

Grasso, M., Lentini, F., 1982. Sedimentary and tectonic evolution of the eastern Hyblean Plateau (southeast Sicily) during late Cretaceous to Quaternary time, Palaeogeogr. Palaeoclimatol. Palaeontol., 39, 261 – 280.

Guidoboni, E., Ferrari, G., Mariotti, D., Comastri, A., Tarabusi, G., Valensise, G., 2007. CFTI4Med, Catalogue of Strong Earthquakes in Italy (461 B.C.–1997) and Mediterranean Area (760 B.C.–1500). INGV-SGA (http://storing.ingv.it/cfti4med).

Gutscher, M.-A., Roger, J., Baptista, M.A., Miranda, J.M., and Tinti, S., 2006. The source of the 1693 Catania earthquake and tsunami (Southern Italy): New evidence from tsunami modeling of a locked subduction fault plane. Geophysical Research Letters, v. 33, n.8, L08309 10.1029/2005GL025442.

Hancock, P.L., 1985. Brittle microtectonics: principles and practice. Journal of Structural Geology 7, 437-457.

Holdsworth, R.E., Strachan, R.A., Magloughlin, J.F., Knipe, R.J. (Eds.), 2001. The Nature and Tectonic Significance of Fault Zone Weakening. Geological Society Special Publication, 186.

Kattenhorn, S.A., Aydin, A., Pollard, D.D., 2000. Joints at high angles to normal fault strike: an explanation using 3-D numerical models of fault-perturbed stress fields. Journal of Structural Geology 22,1-23.

Kim, Y.S., Sanderson, D.J., 2004. The relationship between displacement and length of faults: a review. Earth-Science Reviews 68 (2005) 317–334.

Koopman, A., Speksnijder, A., Horsfield, W.T., 1987. Sandbox model studies of inversion tectonics. Tectonophysics 137, 379–388.

Lavecchia, G., Ferrarini, F., de Nardis, R., Visini, F., Barbano, M.S., 2007a. Active thrusting as a possible seismogenic source in Sicily (southern Italy): Some insights from integrated structural-kinematic and seismological data. Tectonophysics 445, 145–167, doi:10.1016/j.tecto.2007.07.007.

Leeder, M., Alexander, J., 1987. The origin and tectonic significance of asymmetrical meander-belts: Sedimentology, v.34 p-217-226.

Letouzey, J., Werner, P., Marty, A., 1990. Fault reactivation and structural inversion. Backarc and intraplate compressive deformations. Example of the eastern Sunsa shelf (Indonesia). Tectonophysics, 183, 341-362. http://dx.doi.org/10.1016/0040-1951(90)90425-8.

Mattia, M., Bruno, V., Cannavò, F., Palano, M., 2012. Evidences of a contractional pattern along the northern rim of the Hyblean Plateau (Sicily, Italy) from GPS data. Geol. Acta 10, 1–9. http://dx.doi.org/10.1344/105000001705.

McClay, K.R., 1995. 2D & 3D analogue modelling of extensional fault structures: templates for seismic interpretation Pet. Geosci., 1, pp. 163–178 http://dx.doi.org/10.1144/petgeo.1.2.163.

Michetti, A.M., 2005. Future trends in paleoseismology: Integrated study of the seismic landscape as a vital tool in seismic hazard analyses: Tectonophysics, v. 408, p. 3–21, doi: 10.1016/j.tecto.2005.05.035.

Monaco, C., Alicata, A., De Guidi, G., Nucifora, S., 2003. Tettonica trascorrente pleistocenica lungo il margine occidentale del Plateau Ibleo (Sicilia sud-orientale). Boll. Soc. Geol. It., 122, 355-364, 10 ff.

Monaco, C., Tortorici, L., 2000. Active faulting in the Calabrian arc and eastern Sicily. J. Geodyn. 29, 407–424.

Monaco, C., Tortorici, L., 1995. Tettonica estensionale quaternaria nell'Arco Calabro e in Sicilia orientale, Studi Geologici Camerti, Volume Speciale, 2, 351–362.

Morley, C.K., 1988. Variable extension in Lake Tanganyika. Tectonics, 7 (4) (1988), pp. 785–801 http://dx.doi.org/10.1029/TC007i004p00785.

Morley, C.K., Nelson, R.A., Patton, T.L., Munn, S.G., 1990. Transfer zones in the East African rift system and their relevance to hydrocarbon exploration in rifts Am. Assoc. Pet. Geol. Bull., 74 pp. 1234–1253.

Musumeci, C., Patanè, D., Scarfì, L., Gresta, S., 2005. Stress directions and shear-wave anisotropy: observations from local earthquakes in Southeastern Sicily, Italy. Bull. Seism. Soc. Amer. 95 (4), 1359–1374.

Musumeci, C., Scarfì, L., Palano, M., Patanè, D., 2014. Foreland segmentation along an active convergent margin: New constraints in southeastern Sicily (Italy) from seismic and geodetic observations, Tectonophysics, http://dx.doi.org/10.1016/j.tecto.2014.05.017.

Neri, G., Barberi, G., Oliva, G., Orecchio, B., 2005. Spatial variations of seismogenic stress orientations in Sicily, south Italy. Phys. Earth Planet. Inter. 148, 175–191.

Nicolich, R., Laigle, M., Hirn, A., Cernobori, L., Gallard, J., 2000. Crustal structure of the Ionian margin of Sicily: Etna volcano in the frame of regional evolution, Tectonophysics, 329, 121–139, doi:10.1016/S0040-1951(00)00192-X.

Nishigami, K., 1987. Clustering structure and fracture process of microearthquake sequences, J. Phys. Earth 35, 425–448.

Palano, M., Ferranti, L., Monaco, C., Mattia, M., Aloisi, M., Bruno, V., Cannavò, F., Siligato, G., 2012. GPS velocity and strain fields in Sicily and southern Calabria, Italy: updated geodetic constraints on tectonic block interaction in the central Mediterranean. J. Geophys. Res. 117. http://dx.doi.org/10.1029/2012JB009254B07401.

Patacca, E., Scandone, P., Giunta, G., Liguori, V., 1979. Mesozoic paleotectonic evolution of the Ragusa zone (southern Sicily). Geol. Roman. 18, 331–369.

Peacock, D.C.P., 2001. The temporal relationship between joints and faults. Journal of Structural Geology 23, 329-341.

Piatanesi, A., and Tinti, S., 1998, A revision of the 1693 eastern Sicily earthquake and tsunami, J. Geophys. Res., 103, 2749–2758.

Ragg, S., Grasso, M., Müller, B., 1999. Patterns of tectonic stress in Sicily from borehole breakout observations and finite element modeling. Tectonics 18 (4), 669–685. http://dx.doi.org/10.1029/1999TC900010.

Rawnsley, K.D., Rives, T., Petit, J.P., Hencher, S.R., Lumsden, A.C., 1992. Joint development in perturbed stress fields near faults. Journal of Structural Geology 14, 939-951.

Richard, P., Krantz, W., 1991. Experiments on fault reactivation in strike–slip mode. Tectonophysics 188, 117–131.

Rovida, A., Camassi, R., Gasperini, P., Stucchi, M., 2011: CPTI11, the 2011 version of the Parametric Catalogue of Italian Earthquakes. INGV, Milano, Bologna, http://emidius.mi.ingv.it/CPTI, DOI:10.6092/INGV. IT-CPTI11.

Rowe, C.A., Thurber, C.H., White, R.A., 2004. Relocation of volcanic event swarms at Soufriere Hills volcano, Montserrat, 1995–1996, Jour. Volc. Geotherm. Res., 134, 199–221.

Scandone, P., Patacca, E., Rodoicic, R., Ryan, W.B.F., Cita, M.B., Rawason, M., Cherzar, H., Miller, E., Mckenzie, J., Rossi, S., 1981. Mesozoic and Cenozoic rocks from Malta Escarpment (Central Mediterranean). A.A.P.G. Bull. 65,1299–1319.

Scarascia, S., Lozej, A., Cassinis, R., 1994. Crustal structure of the Ligurian, Tyrrhenian and Ionian seas and adjacent onshore areas interpreted from wide-angle seismic profiles. Boll. Geof. Teor. Appl. 36 (141–144), 1–19.

Scarfì, L., Langer, H., Gresta, S., 2003. High-precision relative locations of two microearthquake clusters in southeastern Sicily, Italy. Bull. Seismol. Soc. Am. 93, 1479–1497.

Scarfì, L., Langer, H., Scaltrito, A., 2005. Relocation of microearthquake swarms in the Peloritani mountains—implications on the interpretation of seismotectonic patterns in NE Sicily, Italy. Geophys. J. Int. 163, 225–237, doi:10.1111/j.1365-246X.2005.02720.x.

Scarfì, L., Messina, A., Cassisi, C., 2013. Sicily and Southern Calabria focal mechanism database: a valuable tool for the local and regional stress field determination. Ann. Geophys. 56 (1), D0109, http://dx.doi.org/10.4401/ag-6109.

Scholz, C.H., 1998. Earthquakes and friction laws. Nature 391, 37–42.

Sibson, R., 1981. "A Brief Description of Natural Neighbor Interpolation," chapter 2 in Interpolating Multivariate Data. New York: John Wiley & Sons. 21–36.

Silverman, B. W., 1986. Density Estimation for Statistics and Data Analysis. New York: Chapman and Hall.

Speranza F., Maniscalco R., Mattei M., Di Stefano A., Butler R.W.H., Funiciello R., 1999. Timing and magnitude of rotations in the frontal thrust systems of south-western Sicily. Tectonics, 18, 1178-1197.

Sylvester, A.G., 1988. Strike-slip faults: Geological Society of America Bulletin, v. 100, p. 1666–1703, doi: 10.1130/0016-7606(1988)100<1666:SSF>2.3.CO; 2. Tectonophysics, doi: 10.1016/j.tecto.2014.11.024.

Torelli L., Grasso M., Mazzoldi G., Peis D., 1998. Plio-Quaternary tectonic evolution and structure of the Catania foredeep, the northern Hyblean Plateau and the Ionian shelf (SE Sicily). Tectonophysics, 298: 209-221.

Tsujiura M., 1983a. Waveform and spectral features of earthquake swarms and foreshocks: in special reference to earthquake prediction. Bull. Earth. Res. Inst. Tokyo Univ. 58, 65–133.

Tsujiura M., 1983b. Characteristic frequencies for earthquake families and their tectonic implications: evidence from earthquake swarms in the Kanto District Japan. Pure Appl. Geophys. 4, 573–600.

Viola, G., Odonne F., Mancktelow, N.S., 2004. Analogue modelling of reverse fault reactivation in strike-slip and transpressive regimes: application to the Giudicarie fault system, Italian Eastern Alps. Journal of Structural Geology 36, 401–418.

Visini, F., De Nardis, R., Barbano, M.S., Lavecchia, G., 2009. Testing the seismogenic sources of the January 11th, 1693 Sicilian earthquake (Io X/XI): insights from macroseismic field simulations. Ital. J. Geosci. 128 (1), 147–156.

Watson, D., 1992. Contouring: A Guide to the Analysis and Display of Spatial Data. London: Pergamon Press.

Wells, D.L., Coppersmith, K.J., 1994. New empirical relationships among magnitude, rupture length, rupture width, rupture area, and surface displacement. Bull. Seismol. Soc. Am., 84, 974-1002.

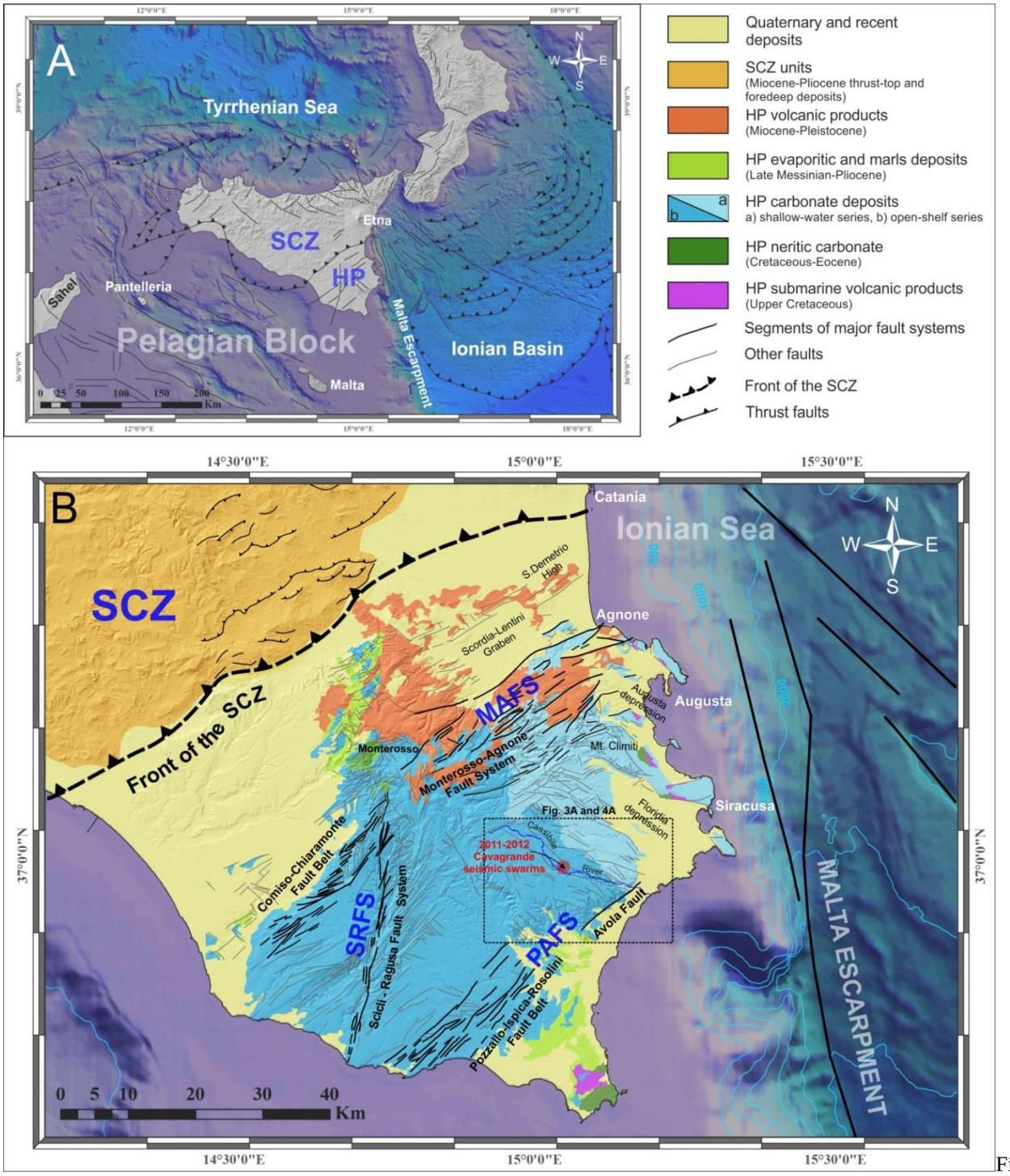

Fig. 1 – A) Tectonic sketch map of the Central Mediterranean area showing the major structural domains with draped the main tectonic boundaries. The Hyblean Plateau (HP) is a portion of the Pelagian Block, a larger continental crustal sector of the Africa margin; B) Geo-structural sketch map of the Hyblean Plateau and its main faults systems (SRFS, Scicli-Ragusa Fault System, MAFS, Monterosso-Agnone Fault System; PAFS, Pozzallo-Avola Fault System); the red circle indicates the area affected by the October 2011-July 2012 Cavagrande Canyon seismic activity. Dashed black line with triangles represents the NE-SW oriented front of the Sicilian Collision Zone (SCZ), a Neogene fold and thrust system that tectonically lies atop the flexured Hyblean succession.

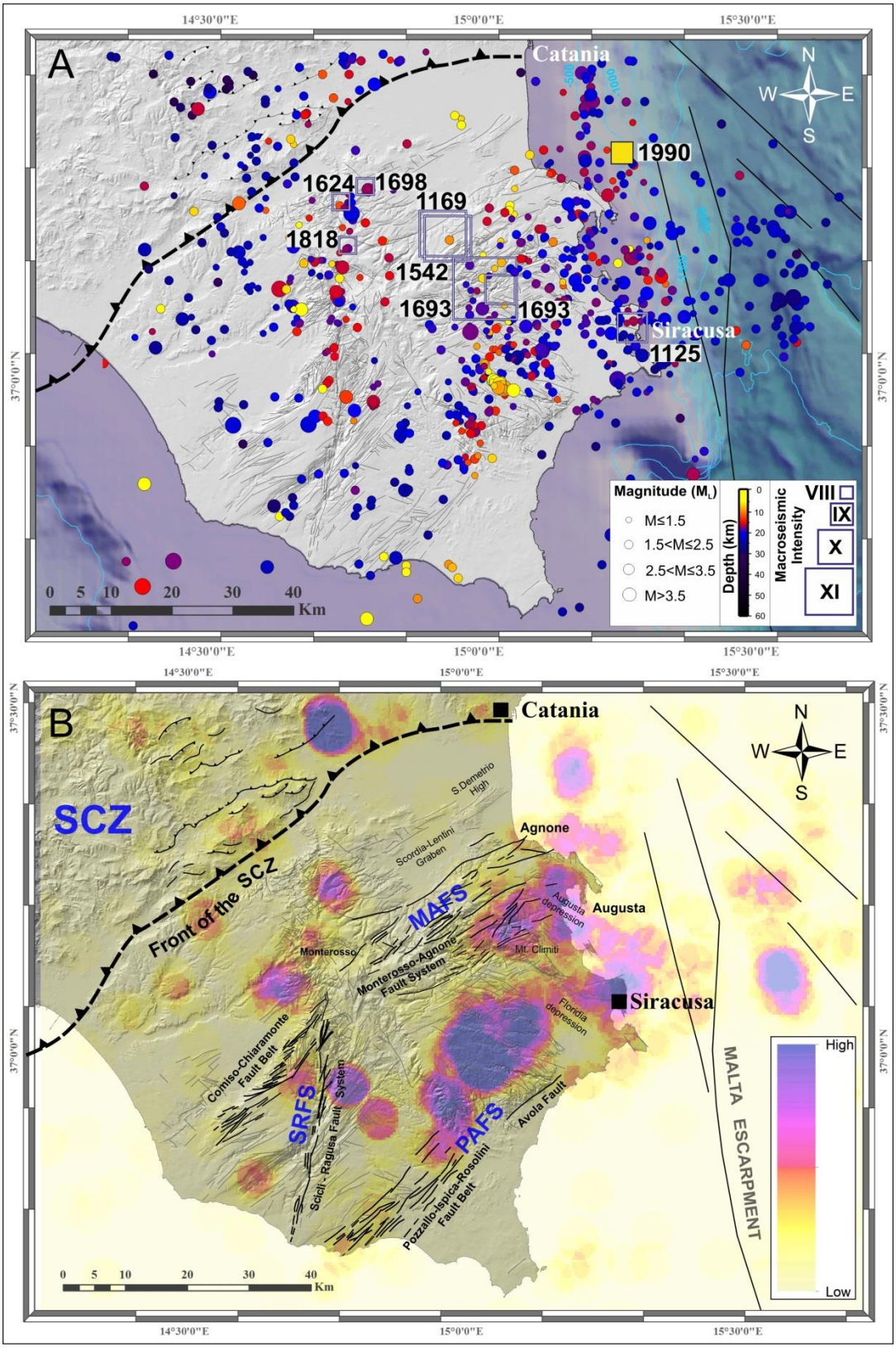

Fig. 2 – A) Location of the instrumental (1994-2013; from Musumeci et al., 2014) and historical (from Guidoboni et al., 2007) earthquakes in the studied area, shown by circles and squares, respectively. The yellow square shows the location of the M_L 5.4 1990 earthquake (from Amato et al., 1995). B) GIS-derived earthquake density map estimated from the 1994 to 2013 by using Kernel density algorithm (Silverman, 1986).

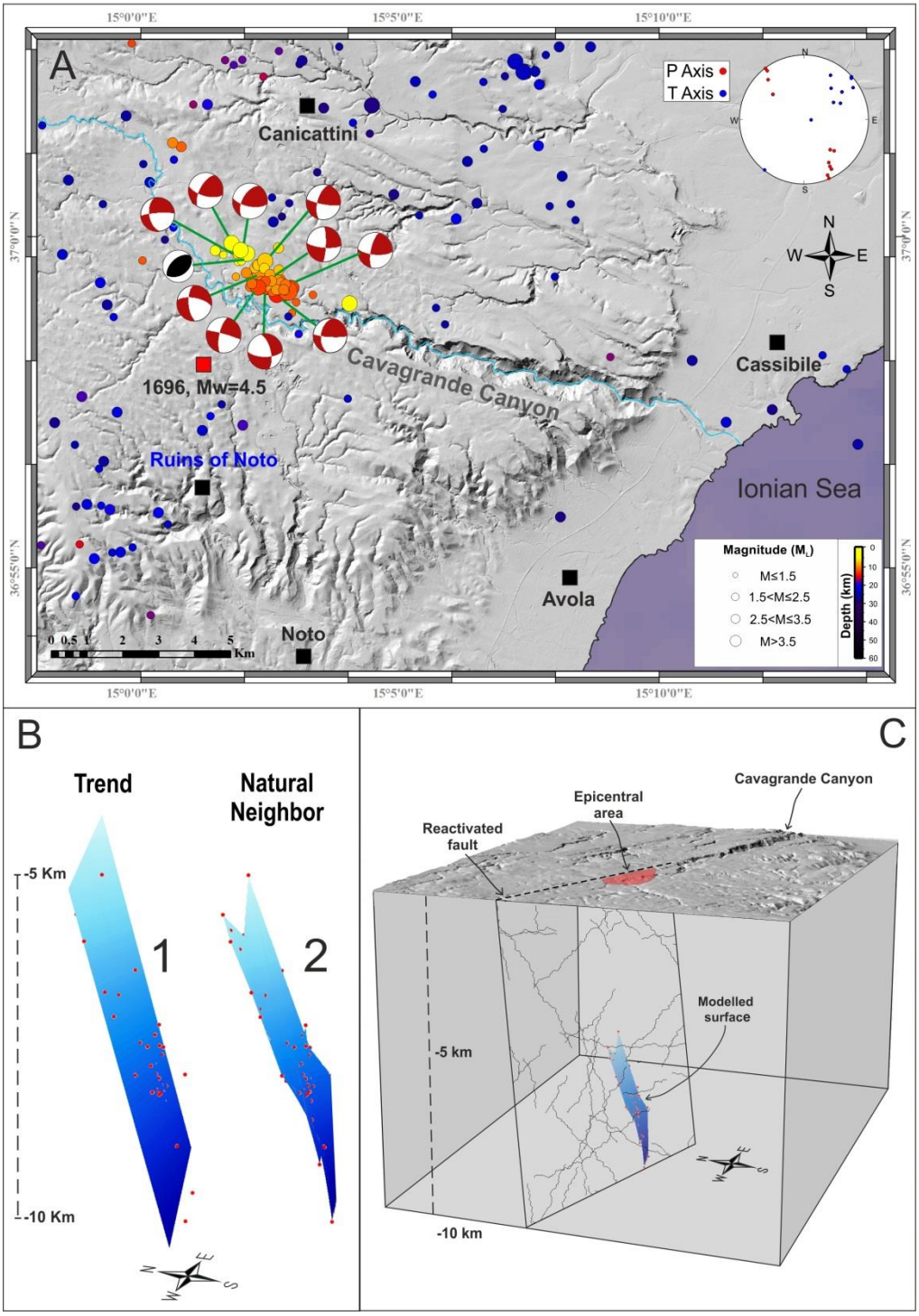

Fig. 3 – A) Map view and focal plane solutions of the earthquakes located in the Cavagrande Canyon area (from Scarfì et al., 2013 and Musumeci et al., 2014). Red, strike-slip mechanism; black, inverse mechanism. In inset the projection of P and T directions computed. The red square indicates the M=4.5 April 20 1696 earthquake. B) Fault plane attitude as modelled from the multiplets hypocentral parameters (x, y and z, the red spheres) identified within the Cavagrande del Cassibile seismic swarms. The interpolation algorithms used (see text for further details) into the GIS platform are 1) "Trend" and 2) "Natural Neighbor" (see Sibson, 1981 and Watson, 1992 for an overview) which provide a ~ 77° dipping, N97-99E oriented surfaces whose ideal updip at surface matches well with the trend of a segment of the Cavagrande Fault Belt (C).

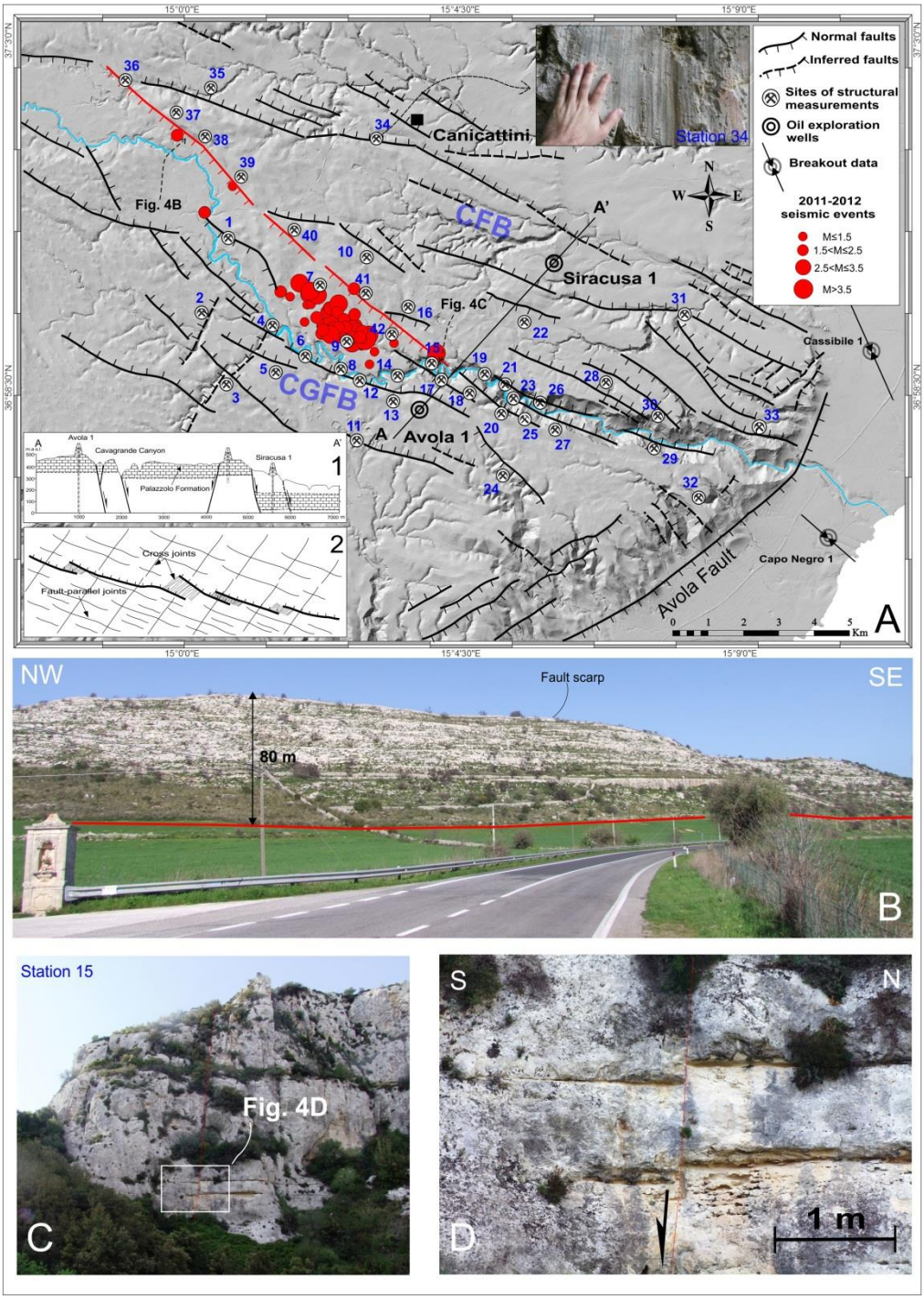

Fig. 4 – (A) Structural map of the area shacked by the 2011-2012 seismic swarms displaying an array of WNW-ESE to NW-SE trending fault segments forming two distinct faults belt, the Cavagrande Faults Belt (CGFB), to the SW, and the Canicattini Faults Belt (CFB), to the NE (see cross section in inset 1 for the their deep-arrangements). The red segments represent the ideal updip at surface of the modelled fault plane (see Fig. 3C). Structural measurements (see the crossed-hammers symbols for location) revealed a pure extensional movement on the CFB with ~90° pitch (photo top-right). The CGFB runs alongside the Cavagrande canyon and it is formed by a suite of left-stepping én-echelon arranged extensional faults strands with antithetic structures. Regions between the discrete segments form relay zones and are characterized by systems of NE-SW striking cross joint (see cartoon in Inset 2 for the reconstructed mutual geometric relations). B) 80 m high fault scarp of the fault segment mapped at the topographic projection of the modelled rupture surface which exhibits a normal motion at its SE tip (C) with a displacement of 0.3 m (D).

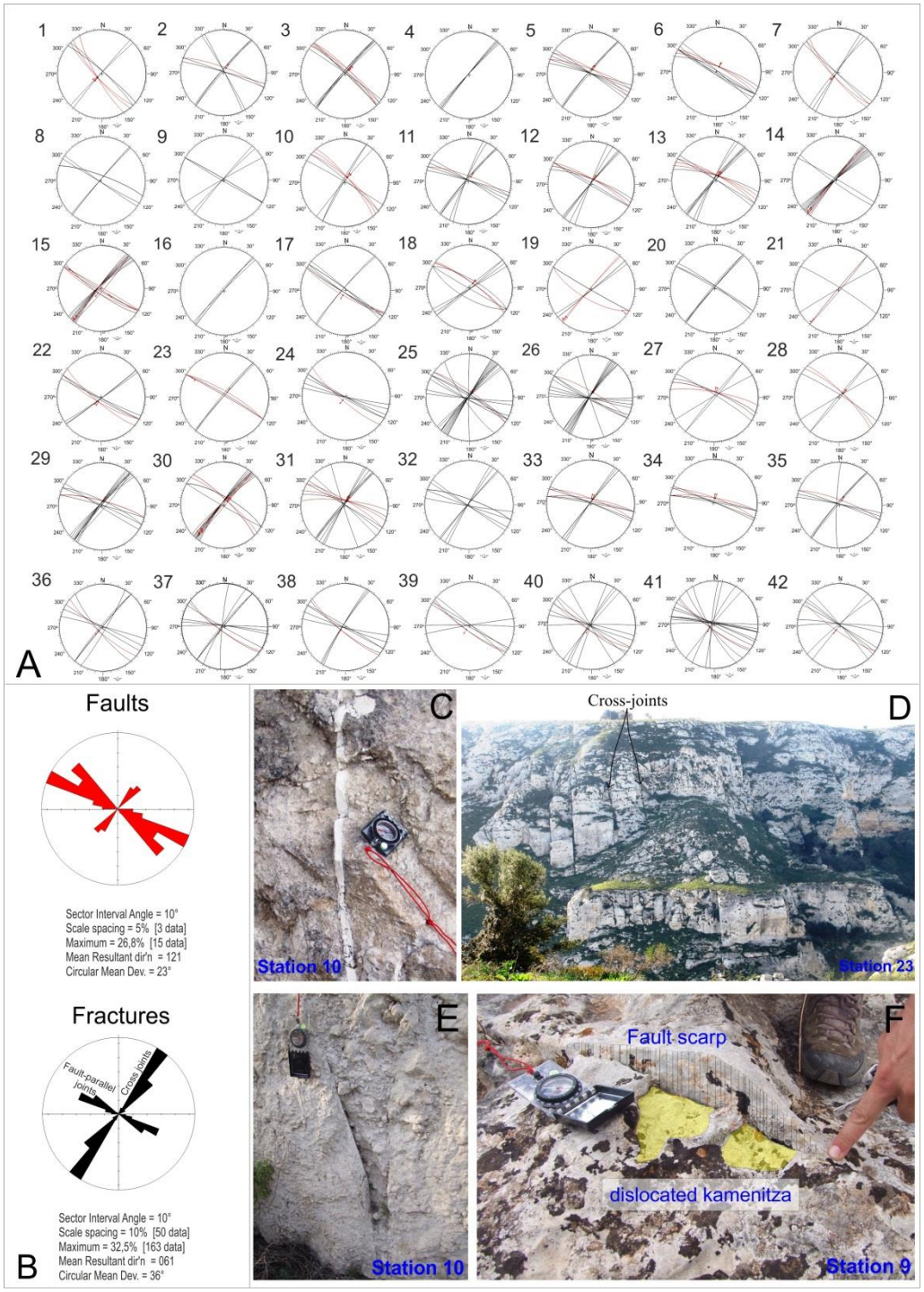

Fig. 5 – A) Stereographic diagrams (Schmidt, lower hemisphere) computed by using Daisy 3 software, showing the planes attitude and kinematics of mesofaults (red) and fractures (black) collected along the investigated area (see fig. 4 for locations). Arrows on fault planes indicate the movement on the respective hanging-wall; B) cumulative rose diagrams showing the azimuthal trend for faults and fractures; C) NE-SW oriented calcite-filled fracture; D) Cross joints measured at site 23. These latter propagates across or terminate against the NW-SE oriented main faults; E) NW-SE oriented Mode I fracture (see text for explanations) recognized at the station 10; F) NE-SW trending dip-slip mesofault displacing a karst morphology (kamenitza).

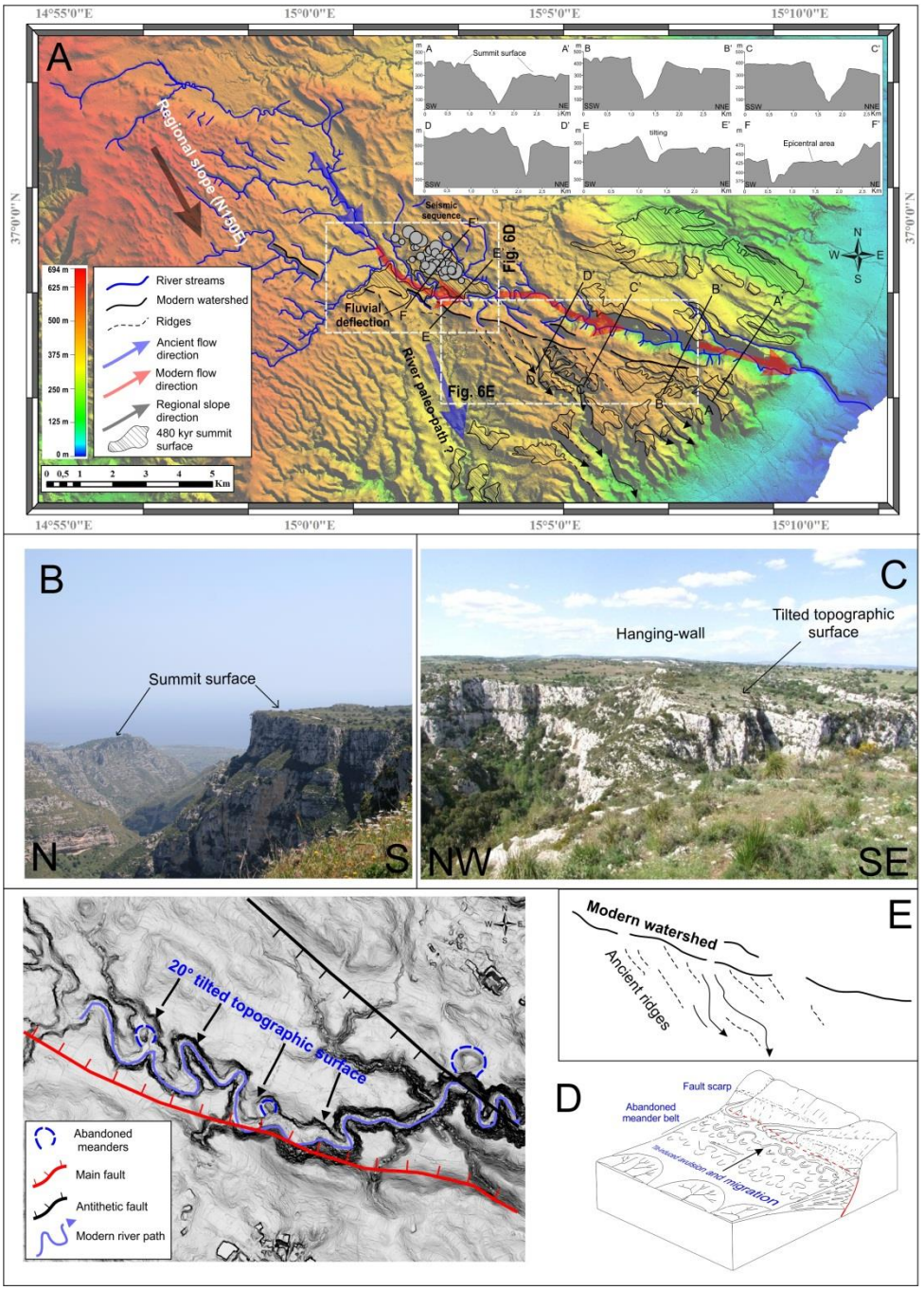

Fig. 6 – A) Main morphological features of the area around the Cavagrande river path obtained by the analysis of an high resolution DTM (2x2 m cell size). The Cassibile river displays a change in fluvial direction from N150E to N105E in correspondence of the area where the seismic sequence nucleated. Topographic profiles (top-right, vertical and horizontal exagg. 3X and 2X respectively) across the canyon highlight a morphological displacement (~50 m) between the northern and southern shoulder of the Cavagrande canyon. This has been related to normal motion along canyon-parallel faults whose activity gave rise also to the offset of the summit surface (B) and ~ 20 tilting along the hanging-walls (C). Tilting towards the fault scarp (D) produced channels migration and a belt of abandoned meanders. E) Canyon-parallel faults have been responsible also for the growth of footwall-ridges that superposed on ancient NW-SE oriented fluvial ridges.

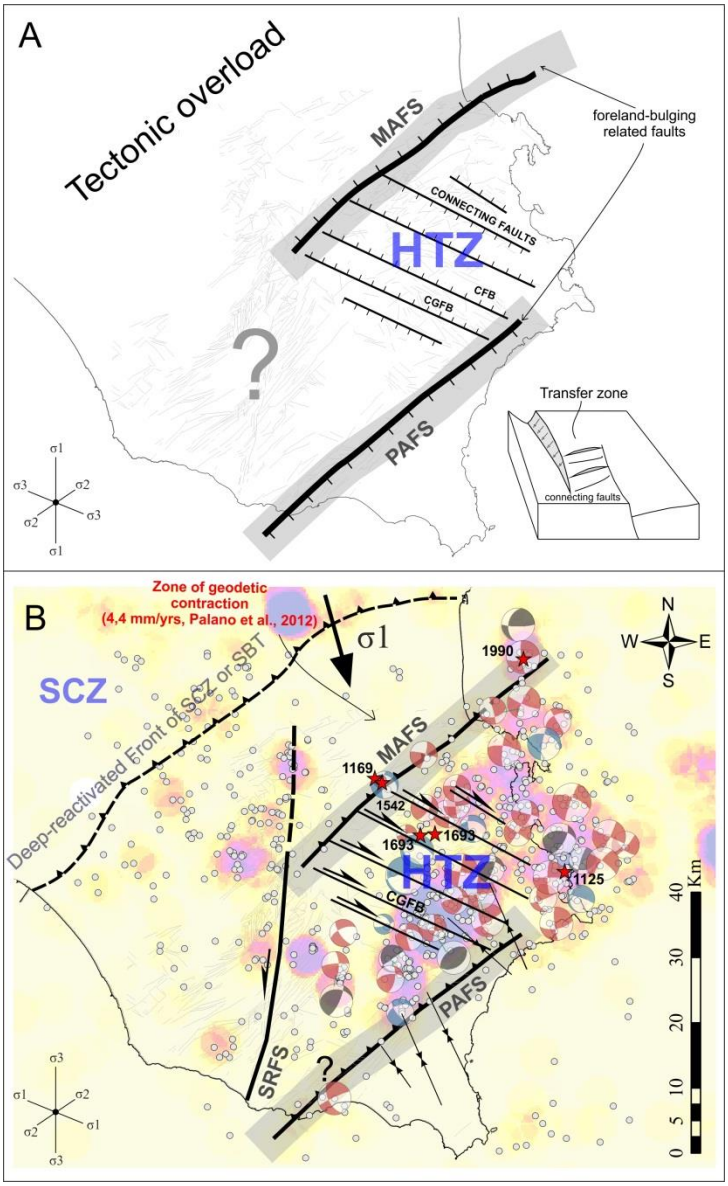

Fig. 7 – A) Tectonic model of the HP during the Neogene-Quaternary time when the tectonic overload by thrust-sheet piling in the SCZ produced bulging of the HP with consequent development of major outer-arc extensional faults systems with opposite dipping, the MAFS and PAFS. These latter probably overlapped forming a transfer zone (the HTZ) composed of connecting extensional fault belts (e.g. the CFB and CGFB) trending ~NW-SE (see model in the right-bottom and text for explanations); B) Present-day deformation model for the HP. The SE migration of deep-seated thrusts in the SCZ according to a sub-horizontal NNW oriented σ1 probably transferred a rate of shortening in the HP with consequent reactivation from normal to reverse along the MAFS and PAFS bounding faults and from normal to right-lateral along the NW-SE oriented connecting faults. This mechanism is corroborated i) by available focal solutions (Musumeci et al., 2014, see the beachballs in the background), ii) by geodetic measurements (Mattia et al., 2012; Palano et al, 2012), which evidenced contraction in the northern border of the HP, and iii) by boreholes breakout data (Ragg et al., 1999, see black opposite arrows), which suggest a possible contraction also along the PAFS. Reverse movements (line with black triangles) along MAFS and PAFS traces indicate only that they should be currently undergoing instrumentally-determined contraction, since evidence of tectonic inversion is not geologically recorded.

Table I –Multiplets source attributes used to reconstruct the fault plane.

Events	Date	Time	Lat	Long	Depth	ML
1	10/6/2011	7:56:42	36.99035	15.04169	7.26442	2.5
2	10/7/2011	21:07:54	36.9894	15.04291	7.61298	2.5
3	10/9/2011	8:28:25	36.99443	15.04025	5.80531	3.3
4	10/9/2011	8:32:01	36.98888	15.04571	7.9605	1.8
5	10/9/2011	8:34:15	36.98846	15.04539	8.17716	1.8
6	10/9/2011	9:50:03	36.98721	15.04677	8.90761	2.4
7	10/9/2011	11:00:18	36.98919	15.04463	7.77309	2.5
8	10/9/2011	11:01:12	36.98869	15.04553	8.039	2.3
9	10/9/2011	11:09:30	36.98887	15.0448	7.83937	2.5
10	10/9/2011	15:42:41	36.9885	15.04373	8.02102	2.2
11	10/9/2011	17:24:59	36.99551	15.03578	5.49437	3
12	10/9/2011	20:32:28	36.98816	15.04404	8.41152	1.8
13	10/9/2011	21:22:58	36.98908	15.04733	7.13734	2.4
14	10/9/2011	22:00:42	36.99013	15.03961	7.73057	2.2
15	10/10/2011	6:12:57	36.9888	15.0457	7.96	2.6
16	10/10/2011	6:18:39	36.99242	15.03775	6.72006	2.8
17	10/10/2011	9:19:19	36.99454	15.03505	5.67815	3.1
18	10/10/2011	13:50:41	36.9867	15.04365	8.78592	1.8
19	10/10/2011	13:58:56	36.99201	15.03902	6.56291	2.7
20	10/11/2011	15:12:28	36.98866	15.04591	8.05752	2.6
21	10/11/2011	19:32:25	36.99224	15.03366	6.42741	1.8
22	10/13/2011	21:00:18	36.99007	15.03718	7.59139	1.7
23	10/13/2011	21:37:39	36.98718	15.04307	9.03462	1.7
24	12/14/2011	4:00:56	36.98846	15.04247	8.00454	1.9
25	6/25/2012	10:52:50	36.99397	15.03636	5.93078	3.1
26	6/25/2012	11:00:22	36.98894	15.04321	7.95887	1.3
27	6/25/2012	11:47:03	36.98606	15.04986	9.73469	1.5
28	6/25/2012	13:22:34	36.98626	15.04514	9.98885	1.5
29	6/27/2012	1:07:38	36.98914	15.04635	7.96125	2.6
30	6/27/2012	1:14:19	36.98654	15.05006	7.92045	3.7
31	6/27/2012	1:20:59	36.98846	15.04702	8.00957	3.1
32	6/27/2012	2:06:12	36.98901	15.04906	7.4996	1.8

931	33	6/27/2012 2:48:01	36.98956	15.04228	7.32977	3.3
932	34	6/27/2012 3:11:22	36.98903	15.04683	7.42214	2.1
933	35	6/27/2012 3:19:54	36.99133	15.04548	6.34791	1.8
934	36	6/27/2012 3:33:09	36.98963	15.0472	7.27938	1.7
935	37	6/27/2012 9:58:34	36.9891	15.04632	7.90989	2.1
936	38	6/27/2012 15:28:35	36.98891	15.04723	7.89577	2.2
937	39	6/27/2012 15:52:57	36.98951	15.0455	7.64478	1.7
938	40	6/27/2012 17:28:37	36.98907	15.04824	7.58815	1.8
939	41	7/2/2012 2:03:34	36.98879	15.04021	7.90795	1.9
940	42	7/5/2012 19:29:12	36.99386	15.0418	5.05769	1.4